

Equatorial and low latitude ionosphere and equatorial spread F

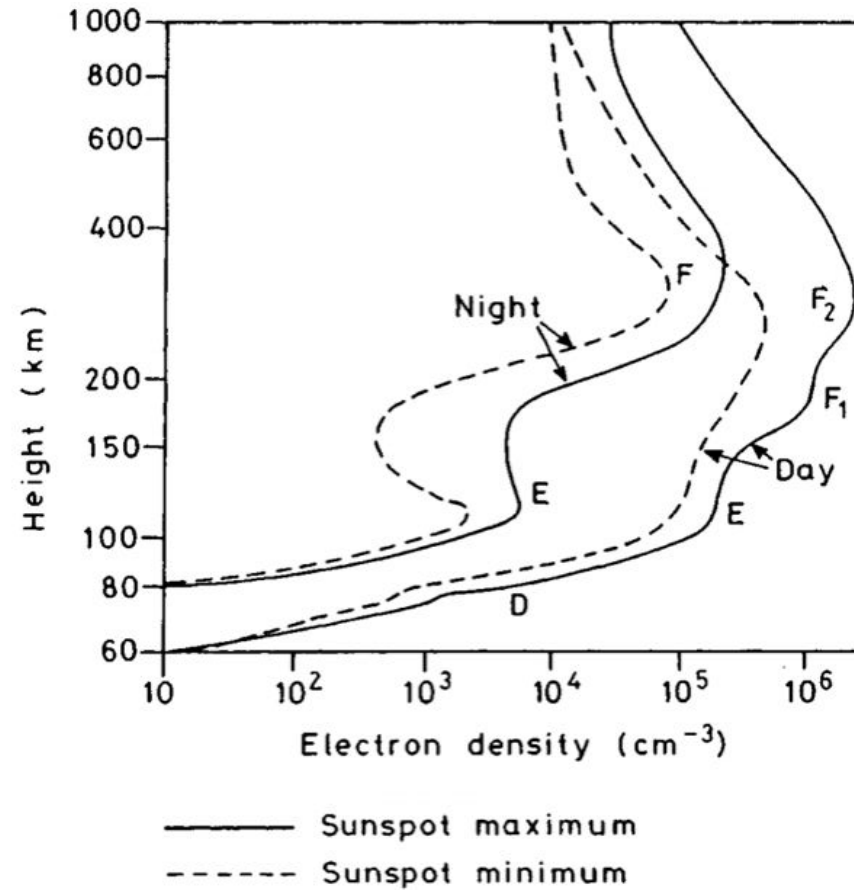
Weijia Zhan

2023/04/19

Outline

- The low-latitude ionosphere
- Vertical plasma drifts and the evening PRE
- The ionospheric Rayleigh-Taylor (RT) instability
- ESF

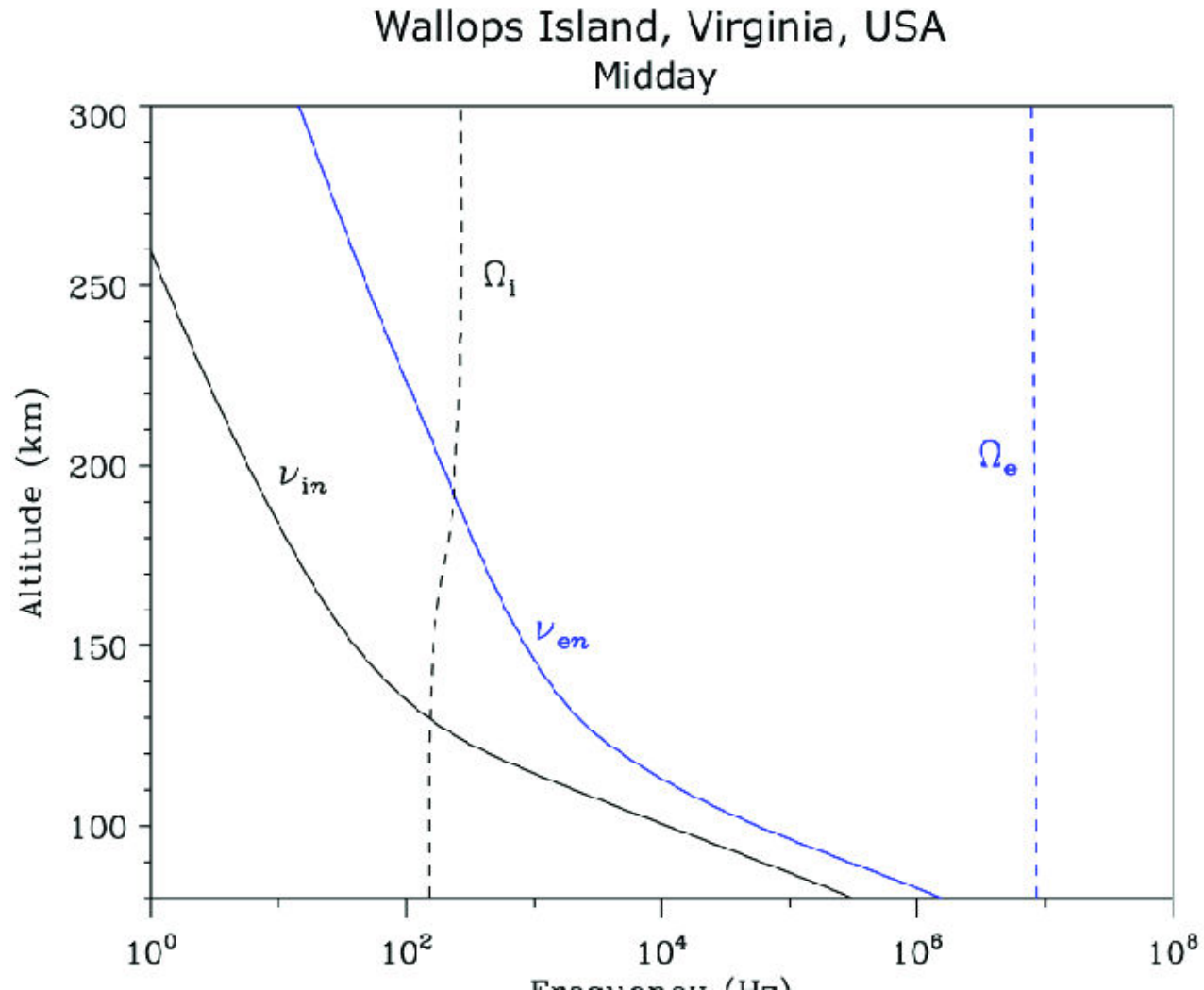
The low-latitude ionosphere



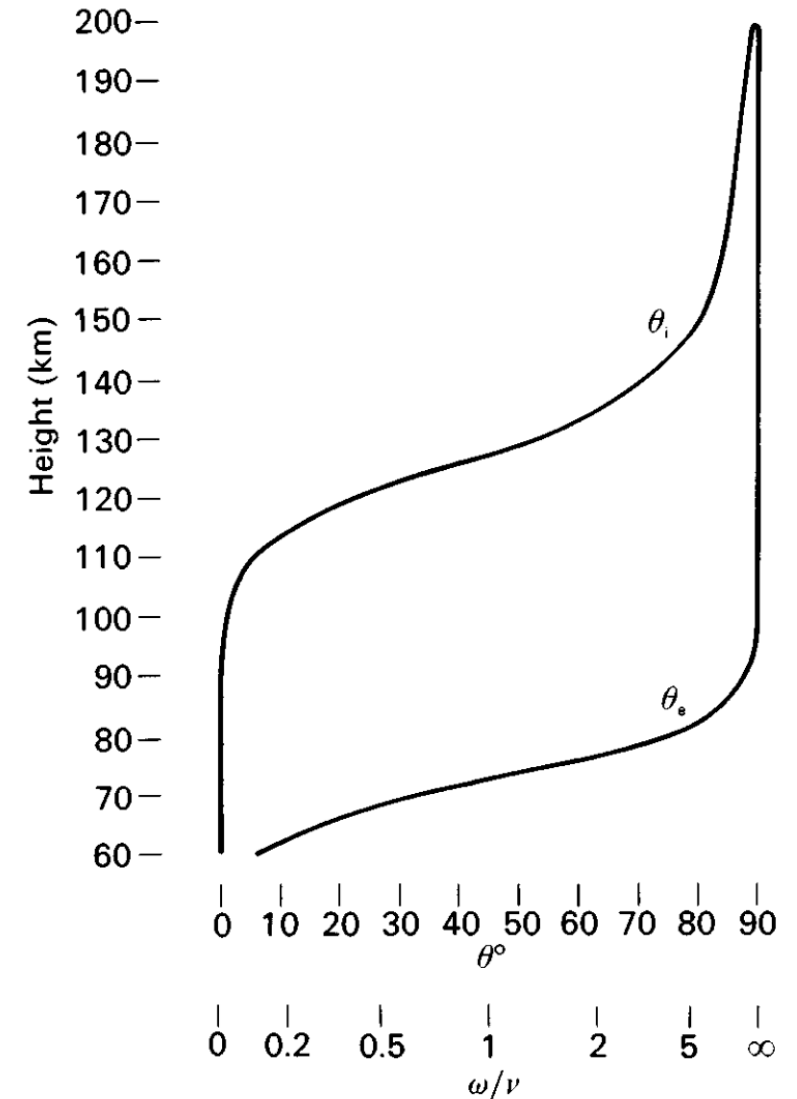
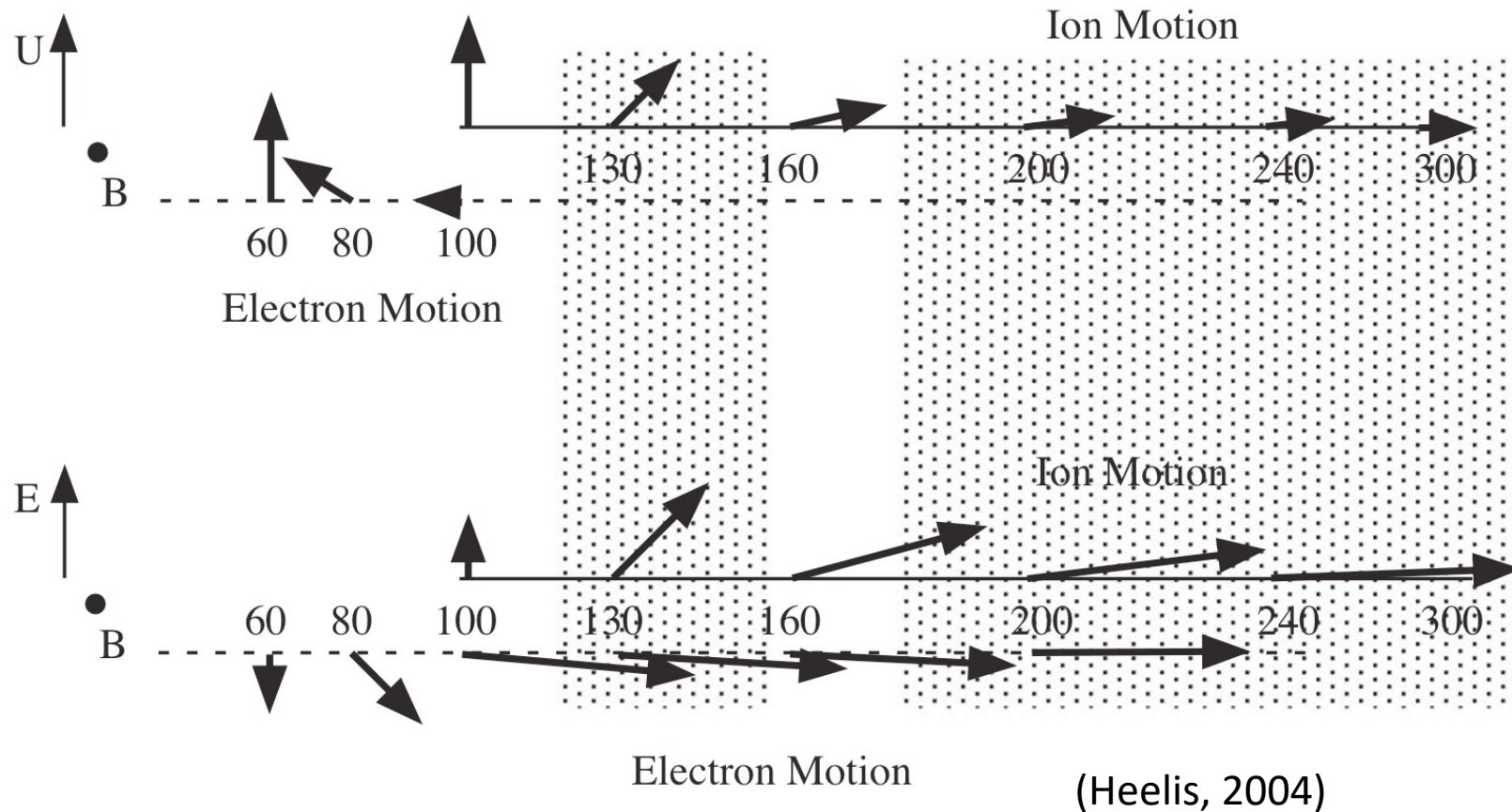
F2: O^+

E, F1: NO^+ , O_2^+

Ion/electron-neutral collision frequency vs gyrofrequency



Plasma motions in the ionosphere



Current and conductivity

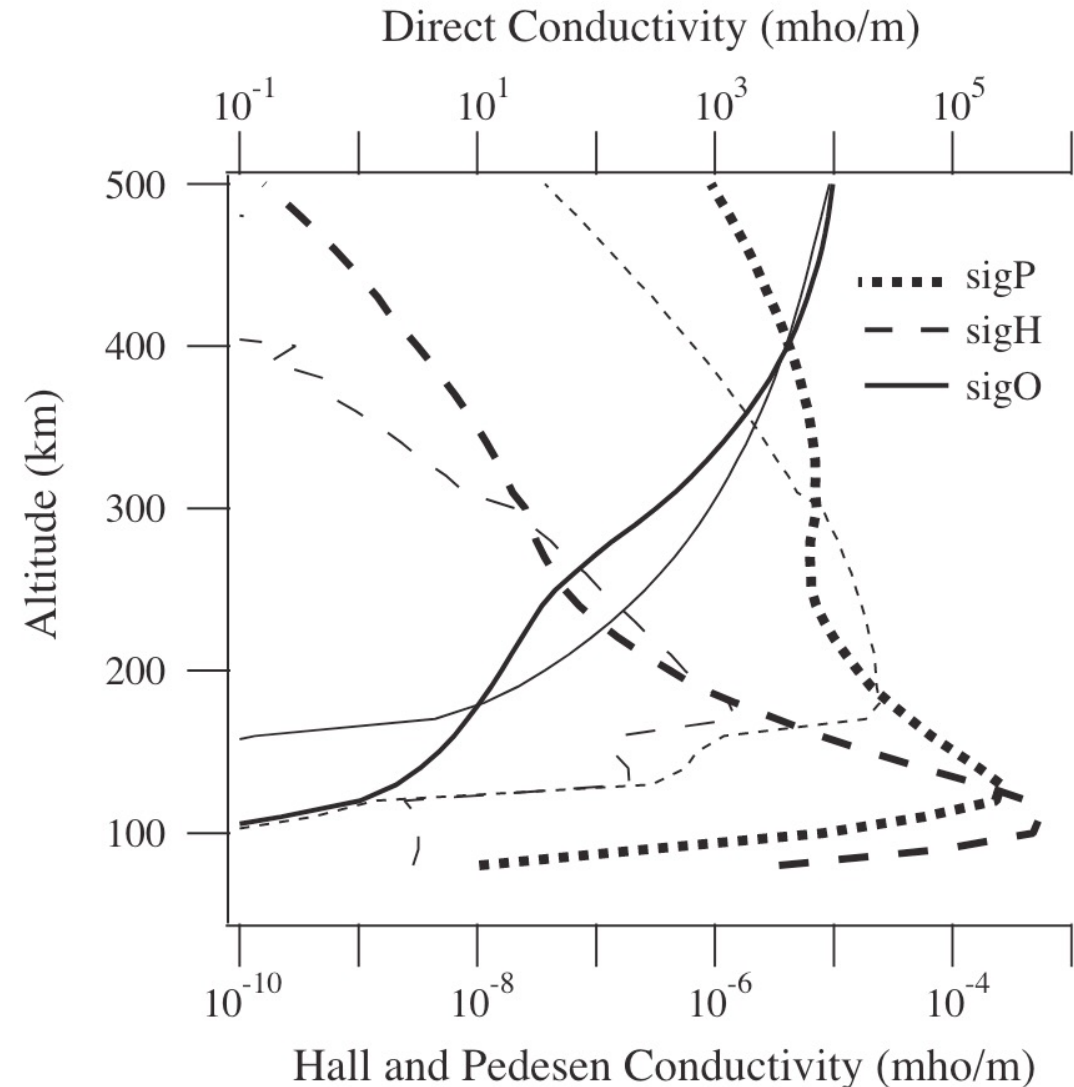
$$\mathbf{j} = N_i e (\mathbf{V}_i - \mathbf{V}_e) = \tilde{\sigma} \frac{\mathbf{F}}{e} = \sigma_0 \frac{\mathbf{F}^{\parallel}}{e} + \sigma_P \frac{\mathbf{F}^{\perp}}{e} - \sigma_H \frac{\mathbf{F}^{\perp} \times \mathbf{b}}{e}.$$

$$\sigma_0 = \frac{Ne^2}{m_e v_e} + \frac{Ne^2}{m_i v_i} \approx \frac{Ne^2}{m_e v_e},$$

$$\sigma_P = Ne^2 \left[\frac{1}{m_e} \frac{v_e}{(v_e^2 + \Omega_e^2)} + \frac{1}{m_i} \frac{v_i}{(v_i^2 + \Omega_i^2)} \right],$$

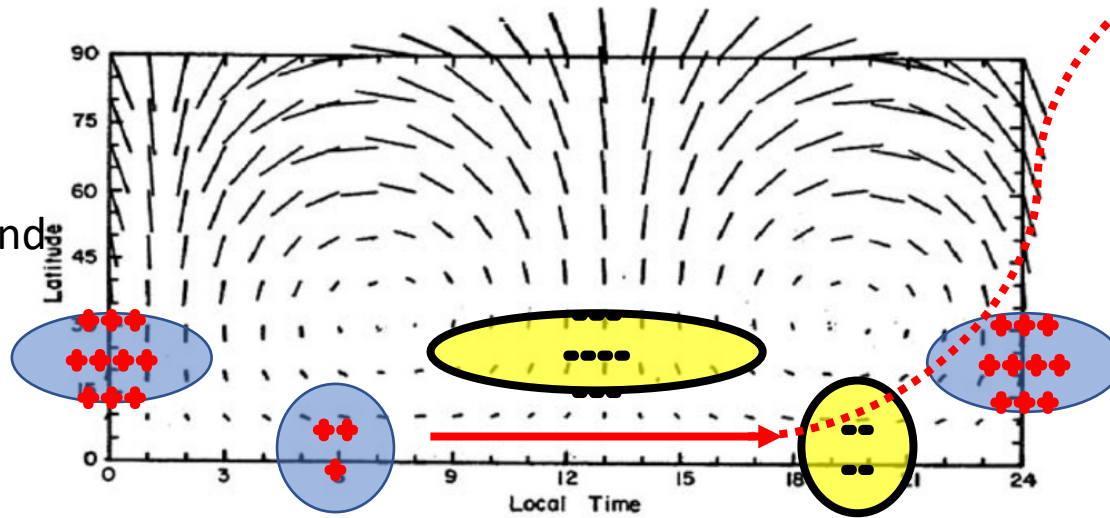
$$\approx \frac{Ne^2}{m_i} \frac{v_i}{(v_i^2 + \Omega_i^2)},$$

$$\sigma_H = Ne^2 \left[\frac{1}{m_e} \frac{\Omega_e}{(v_e^2 + \Omega_e^2)} - \frac{1}{m_i} \frac{\Omega_i}{(v_i^2 + \Omega_i^2)} \right].$$

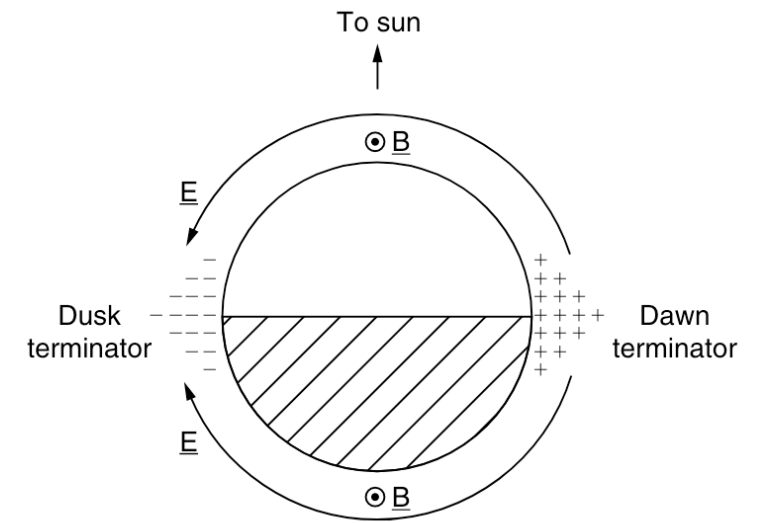
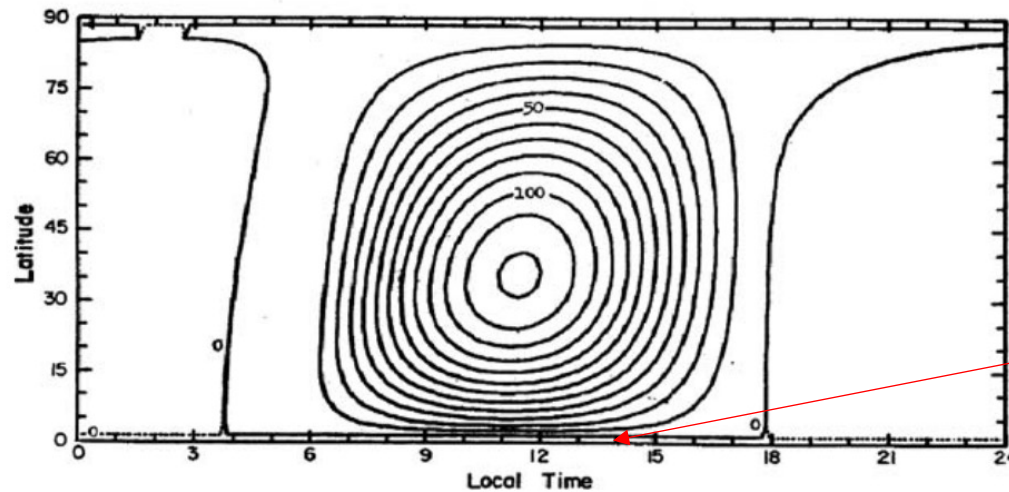


E region dynamo

Neutral wind



Current



$$\begin{array}{c}
 \begin{array}{c} \hat{E}_z \hat{a}_z \\ \uparrow \\ \underline{B} \otimes \end{array} \rightarrow \begin{array}{c} \hat{E}_x \hat{a}_x \\ \rightarrow \end{array} \\
 \hline
 \begin{array}{c} \sigma \approx 0 \\ \sigma \neq 0 \\ \sigma \approx 0 \end{array} \downarrow \begin{array}{c} \sigma_H E_x \\ \sigma_P E_z \end{array} \uparrow \begin{array}{c} \sigma_P E_z \\ \sigma_H E_x \end{array} \rightarrow \begin{array}{c} J_x = \sigma_P E_x + \sigma_H E_z \\ J_z = -\sigma_H E_x + \sigma_P E_z = 0 \end{array}
 \end{array}$$

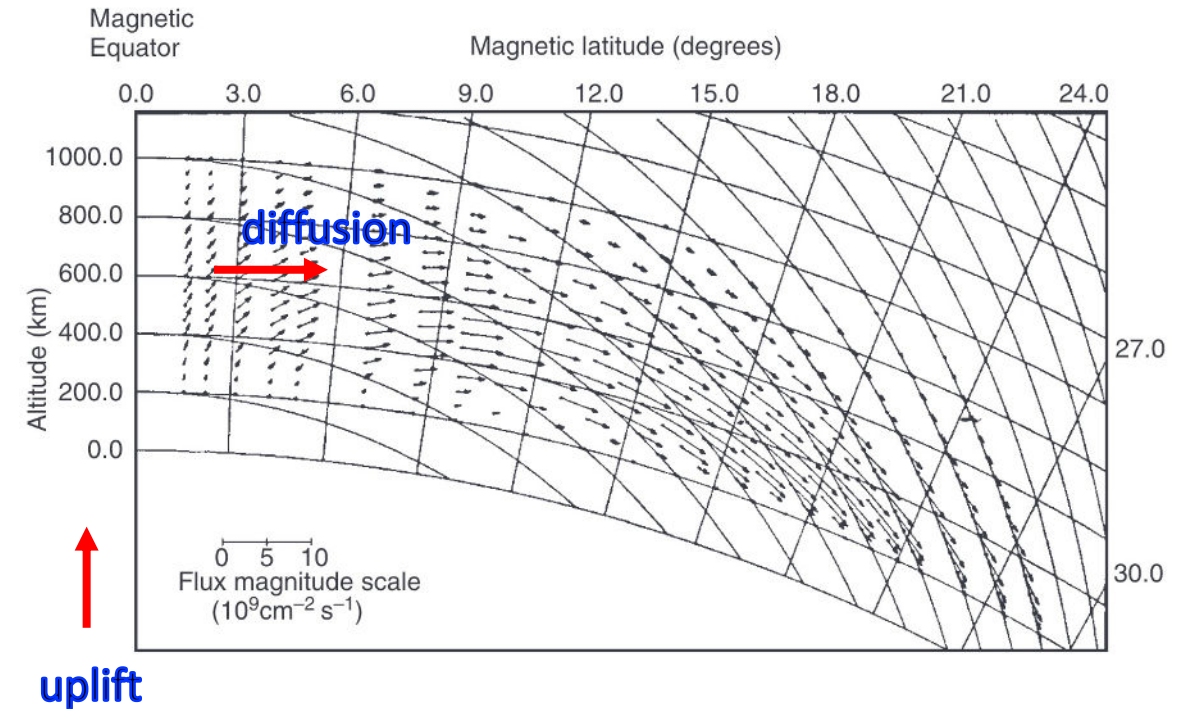
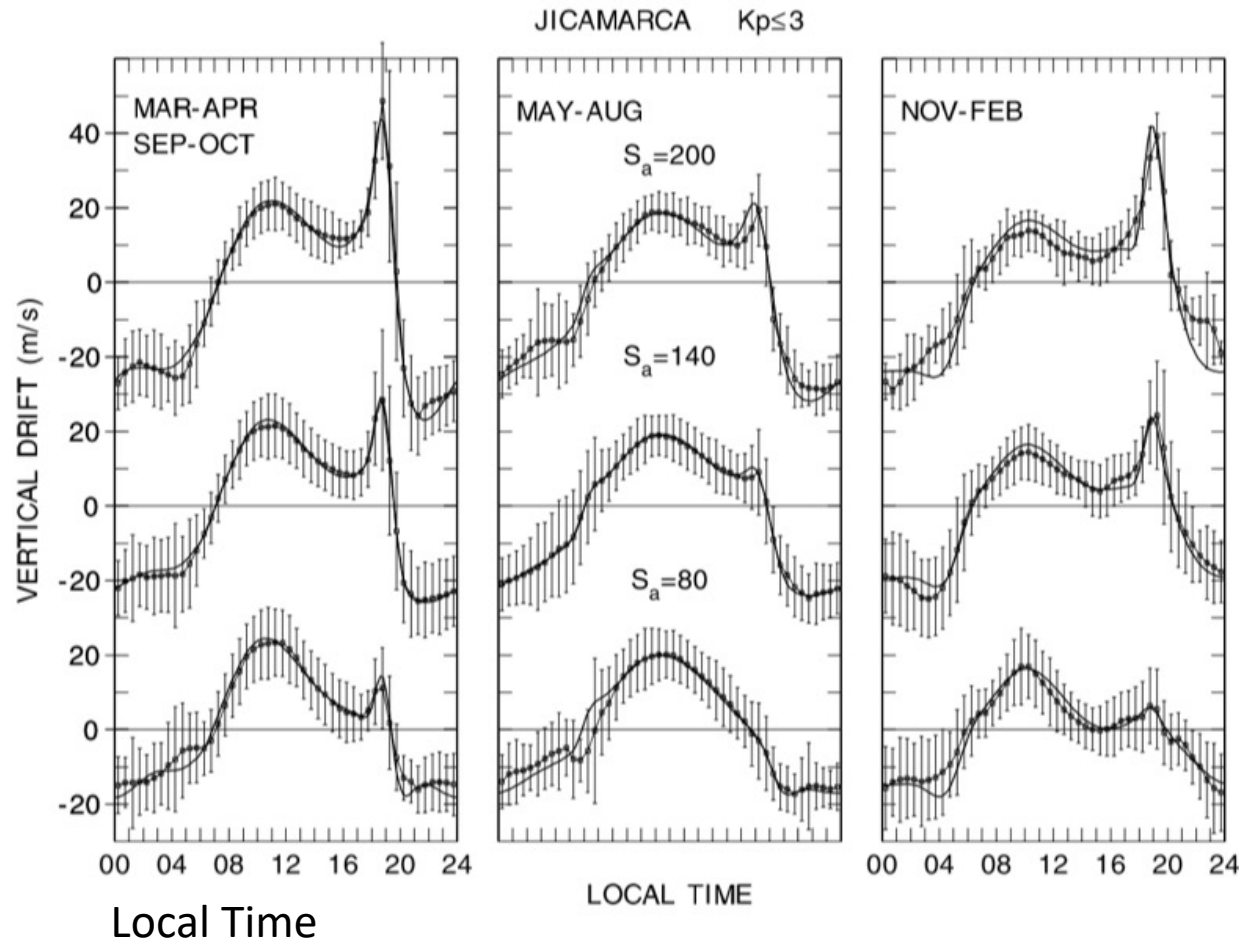
The equatorial electrojet in a slab geometry.

Equatorial electrojet

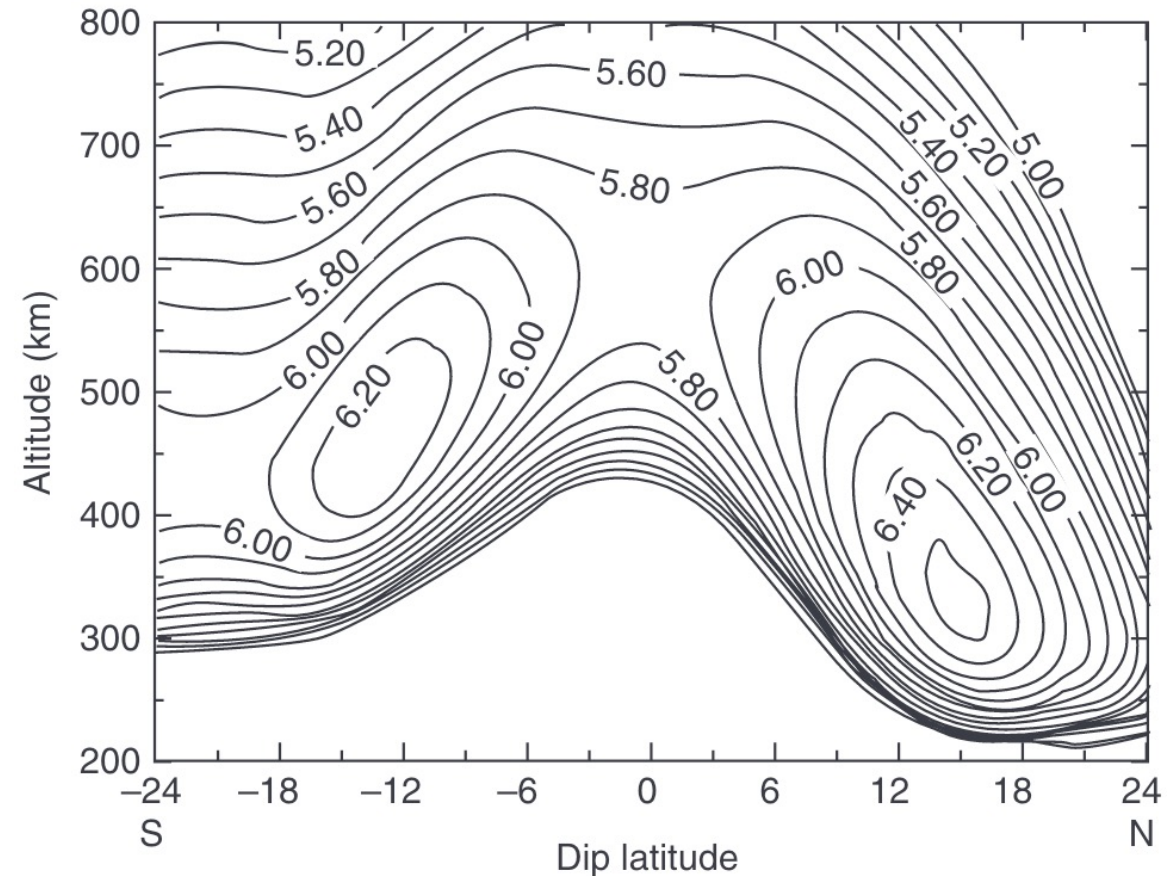
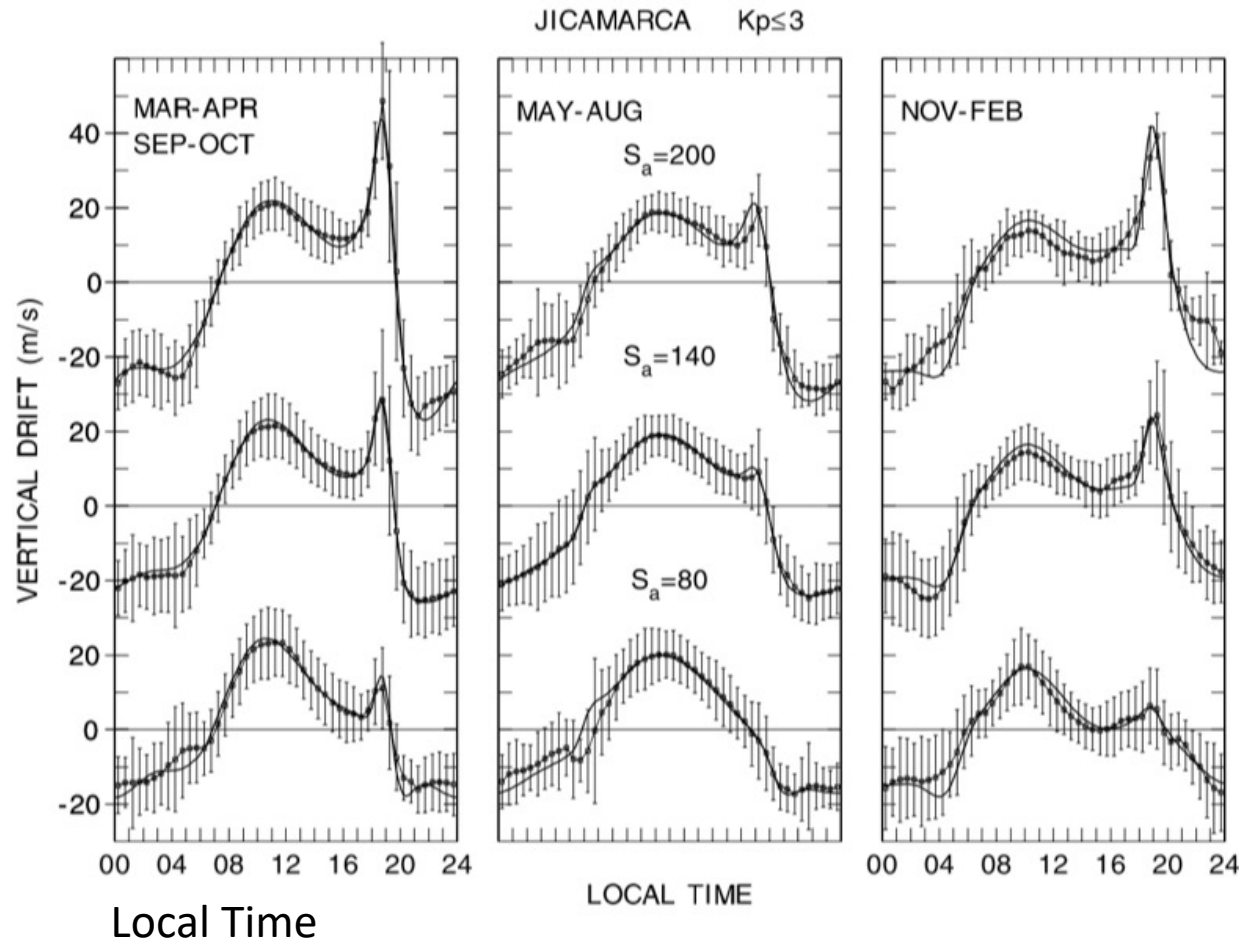
Observed by ground-based magnetometer at the equator.

(Tarpley, 1970)

Vertical drifts and equatorial ionization anomaly



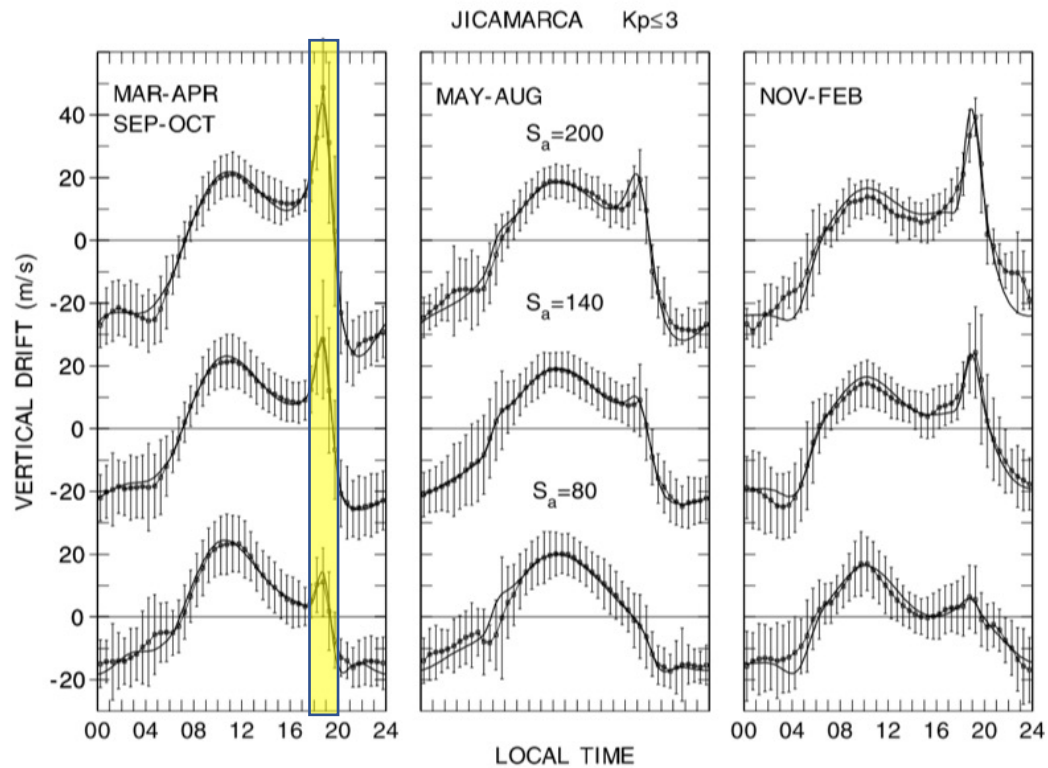
Vertical drifts and equatorial ionization anomaly



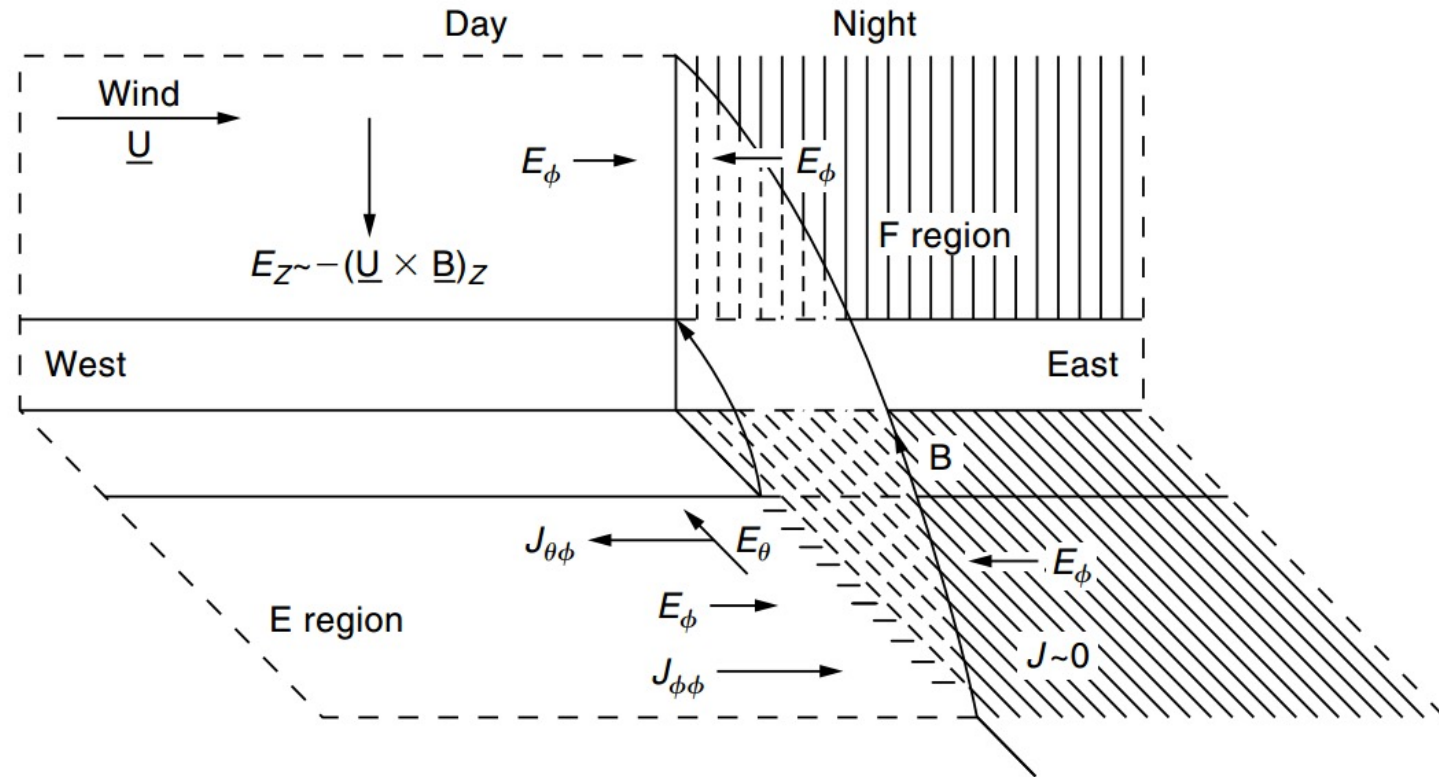
EIA

Vertical drifts and F region dynamo

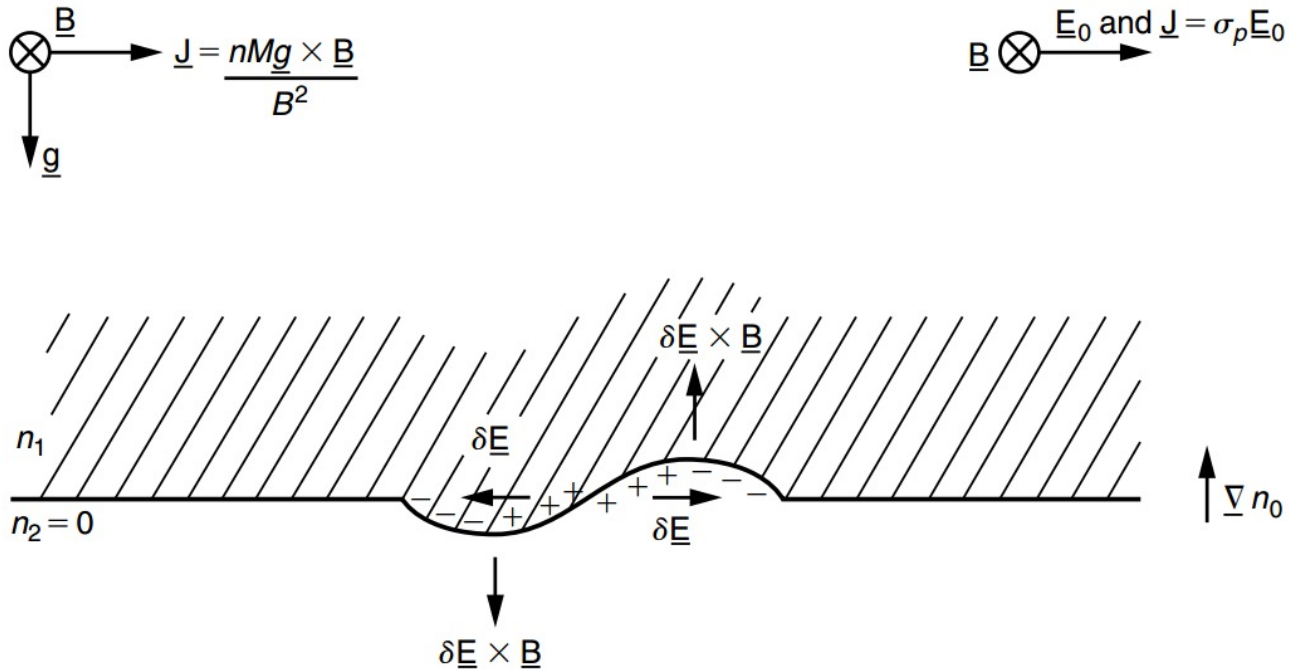
$$\mathbf{E} = \frac{\Sigma_F^p}{\Sigma_E^p + \Sigma_F^p} (\mathbf{U}_F \times \mathbf{B}).$$



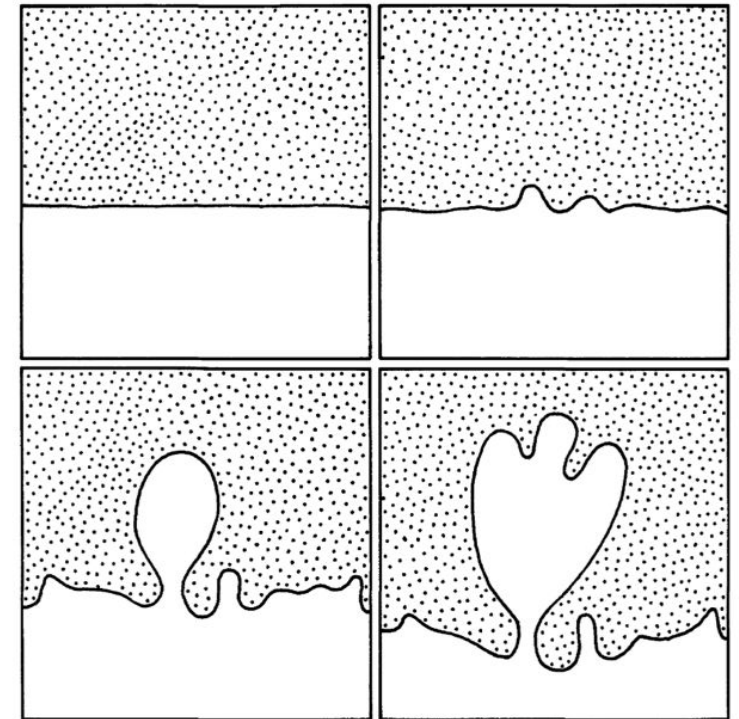
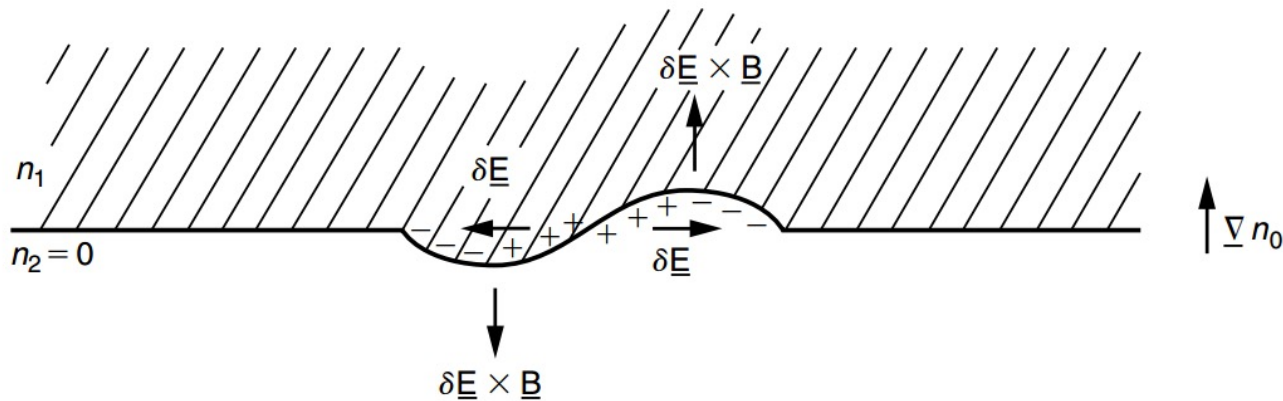
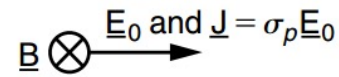
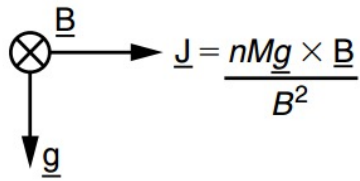
Pre-reversal enhancement (PRE)



The ionospheric Rayleigh-Taylor instability

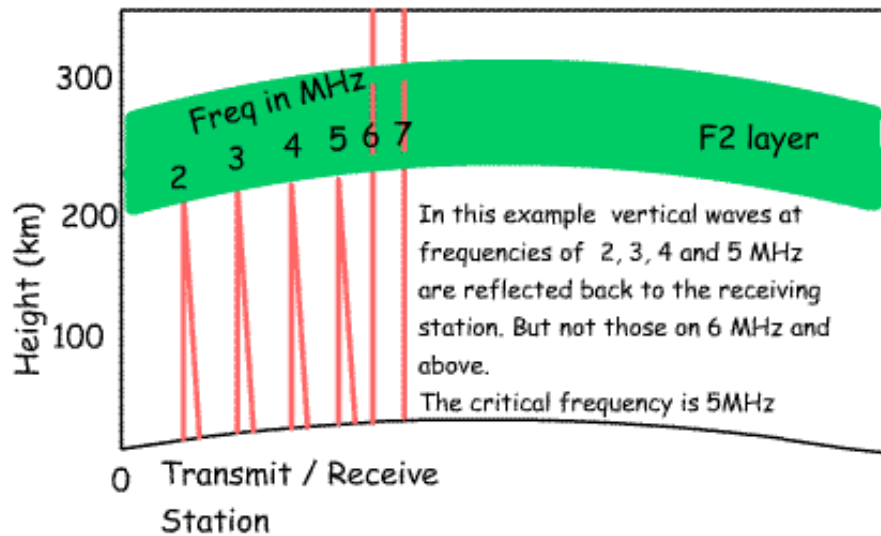


The ionospheric Rayleigh-Taylor instability

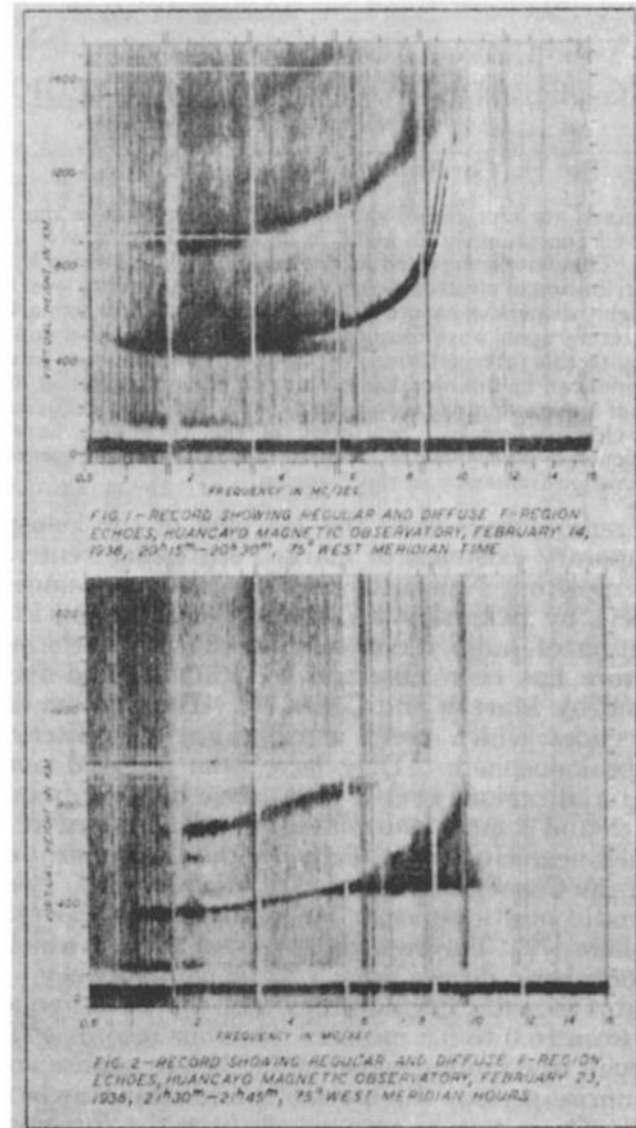


Equatorial spread F: ionosonde and ionogram

Ionospheric propagation - critical frequency



$$f_c \approx 9\sqrt{N_{max}}$$



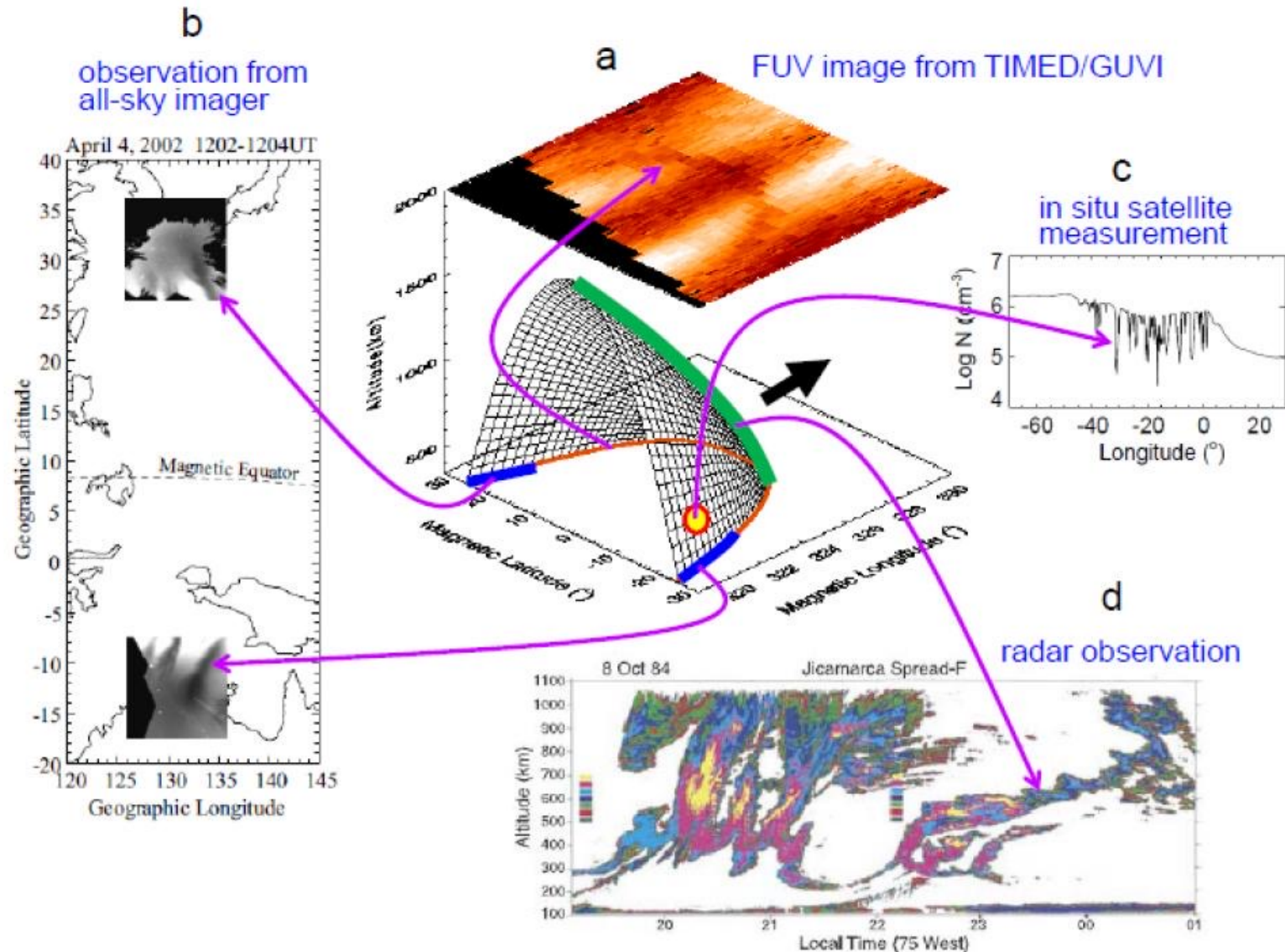
Range spread

Frequency spread

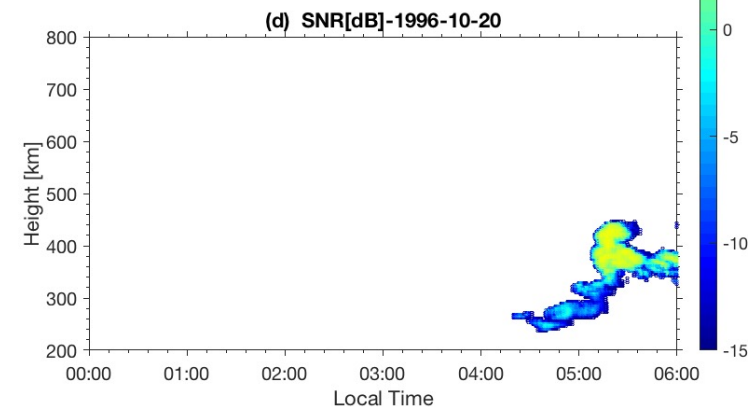
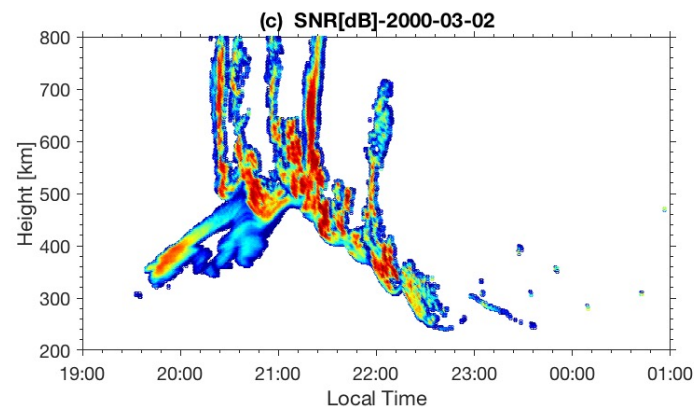
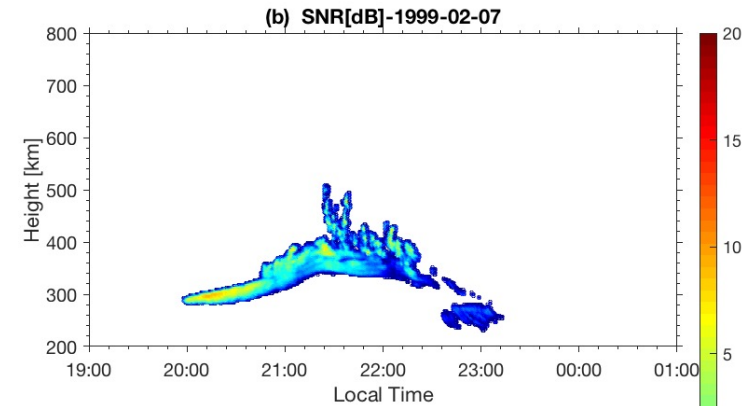
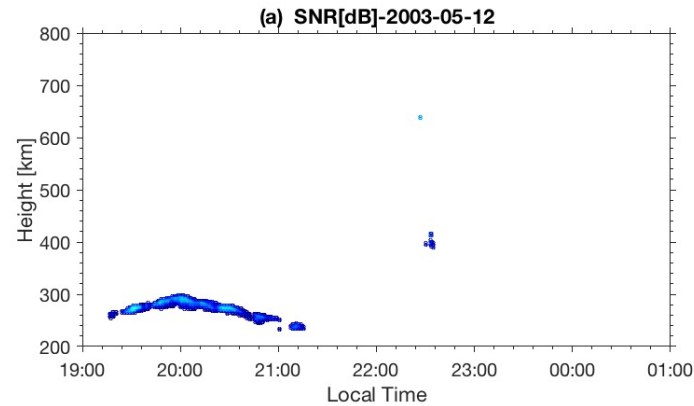
(Booker & Wells, 1938)

Observation of ESF

The peak of the volumetric emission rate occurs in the bottomside *F*-region and is proportional to the product between O^+ and O_2 densities.



Types of radar equatorial spread F (ESF)



Controlling factors

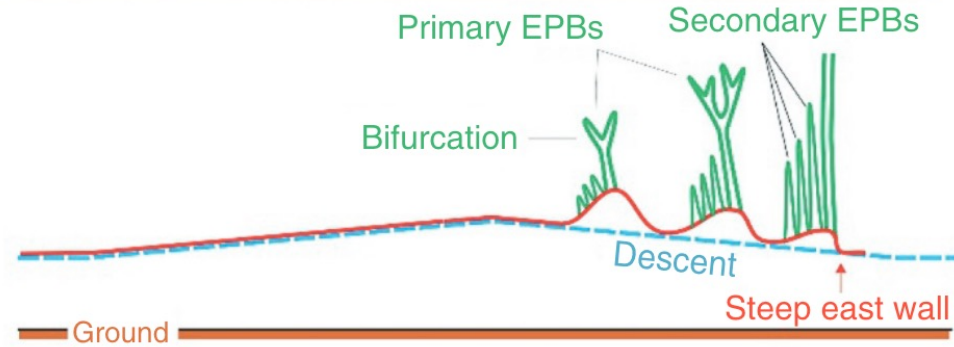
Linear growth rate of generalized RT instability

$$\gamma_{GRT} = \frac{\Sigma_P^F}{\Sigma_P^E + \Sigma_P^F} \left(V_P - U_L^P + \frac{g_e}{\nu_{eff}} \right) K^F - R$$

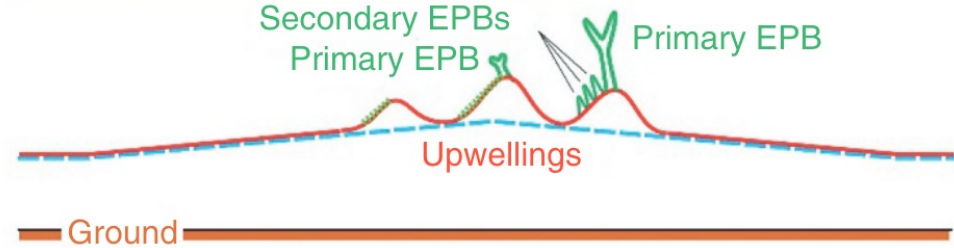
(Sultan, 1996)

vertical drift meridional wind ion-neutral collision frequency Electron density gradient Recombination

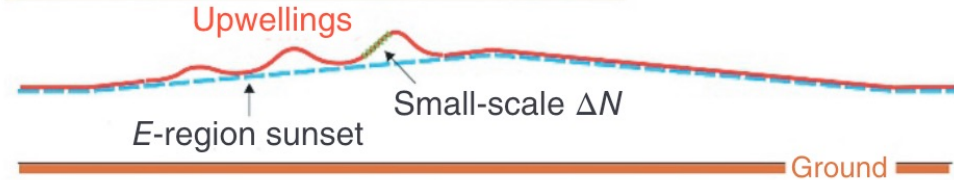
(d) Stage 4: Evolution and decay (descent of F layer)



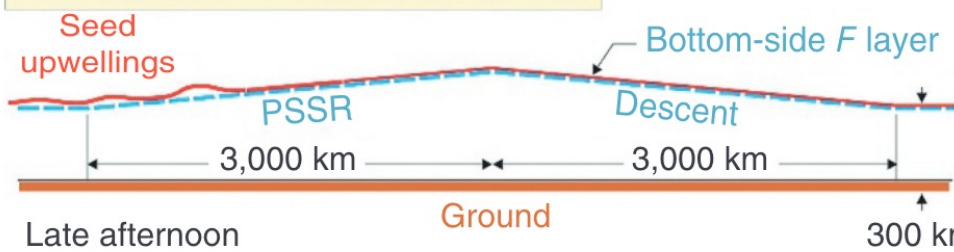
(c) Stage 3: EPB development (SS_F)



(b) Stage 2: Upwelling growth (SS_E)



(a) Stage 1: Seed (late afternoon)

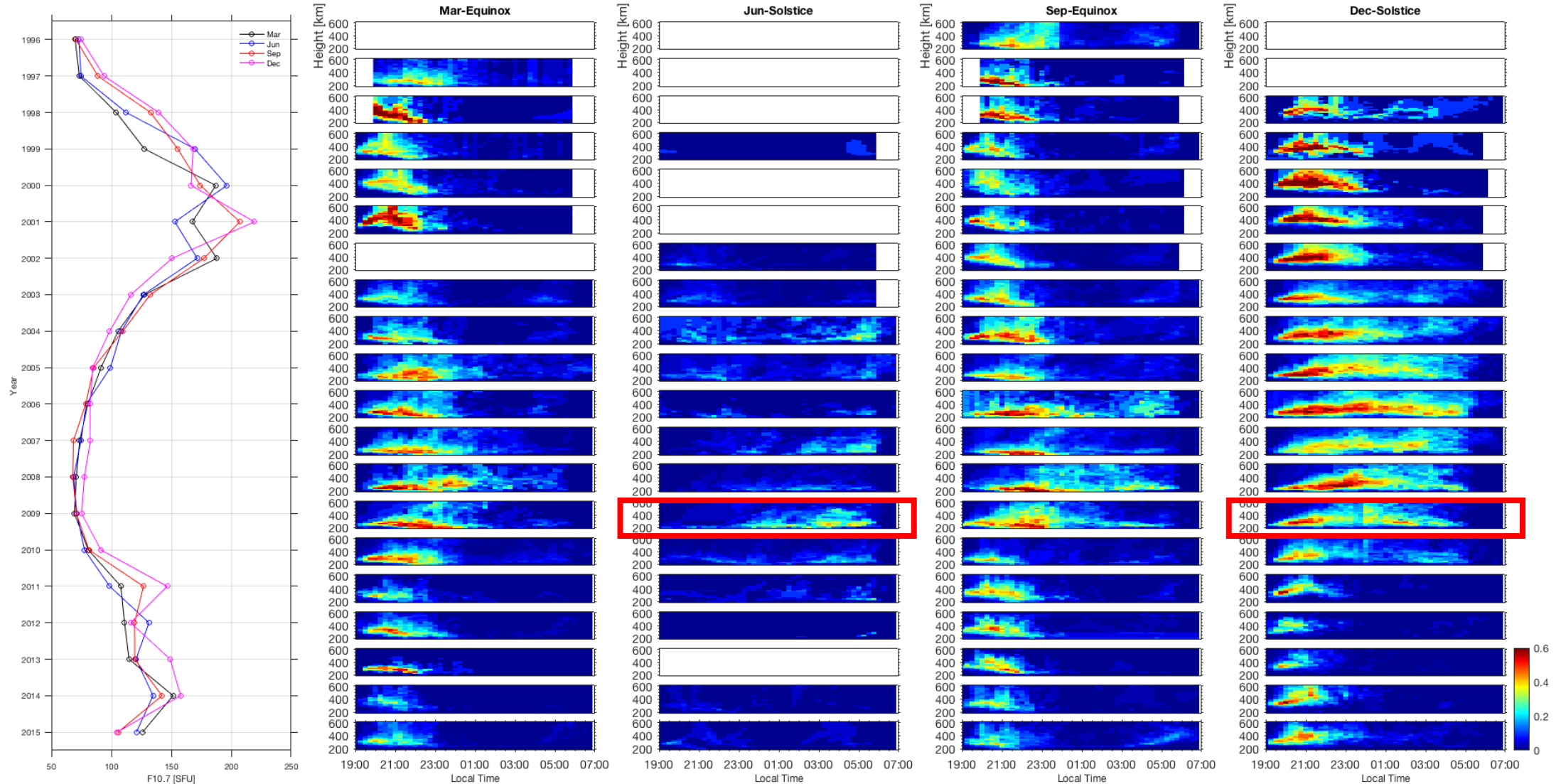


(Tsunoda, 2021)

Climatology of occurrence rate

1996

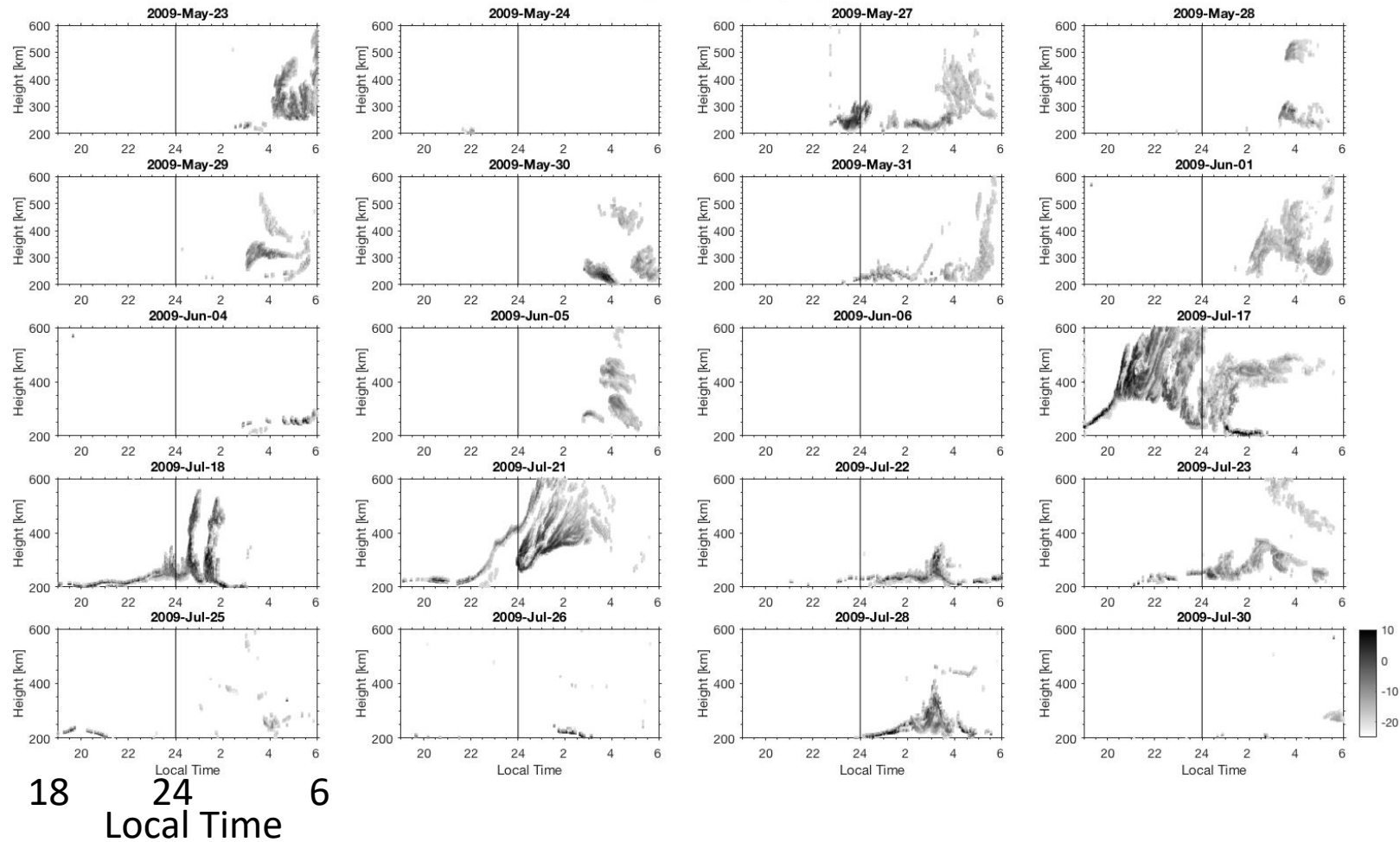
2015



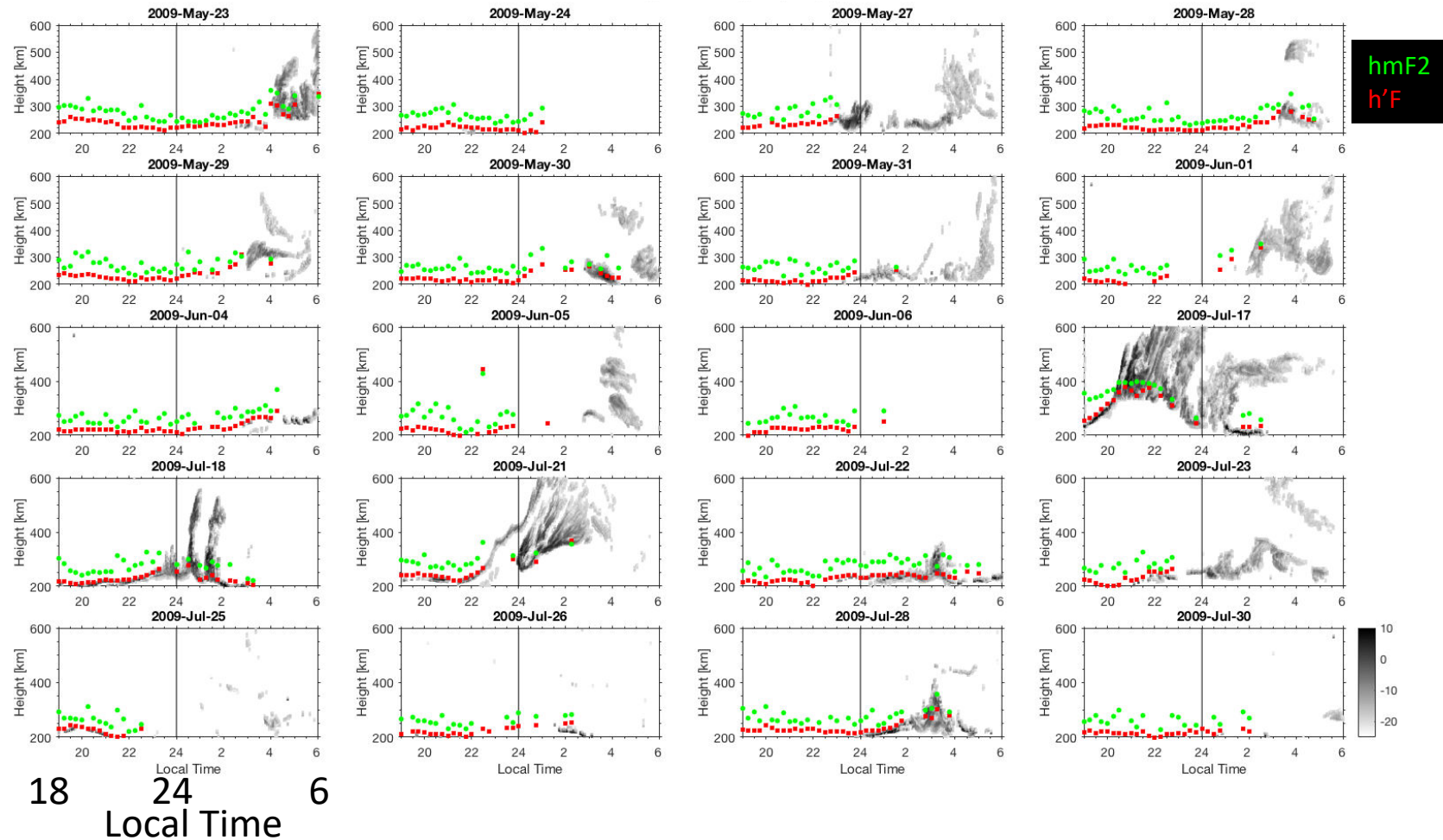
Postmidnight ESF

- June Solstice ESF: Morphology
- ✓ ESF occurs, predominantly, in the post-midnight sector

RTI map

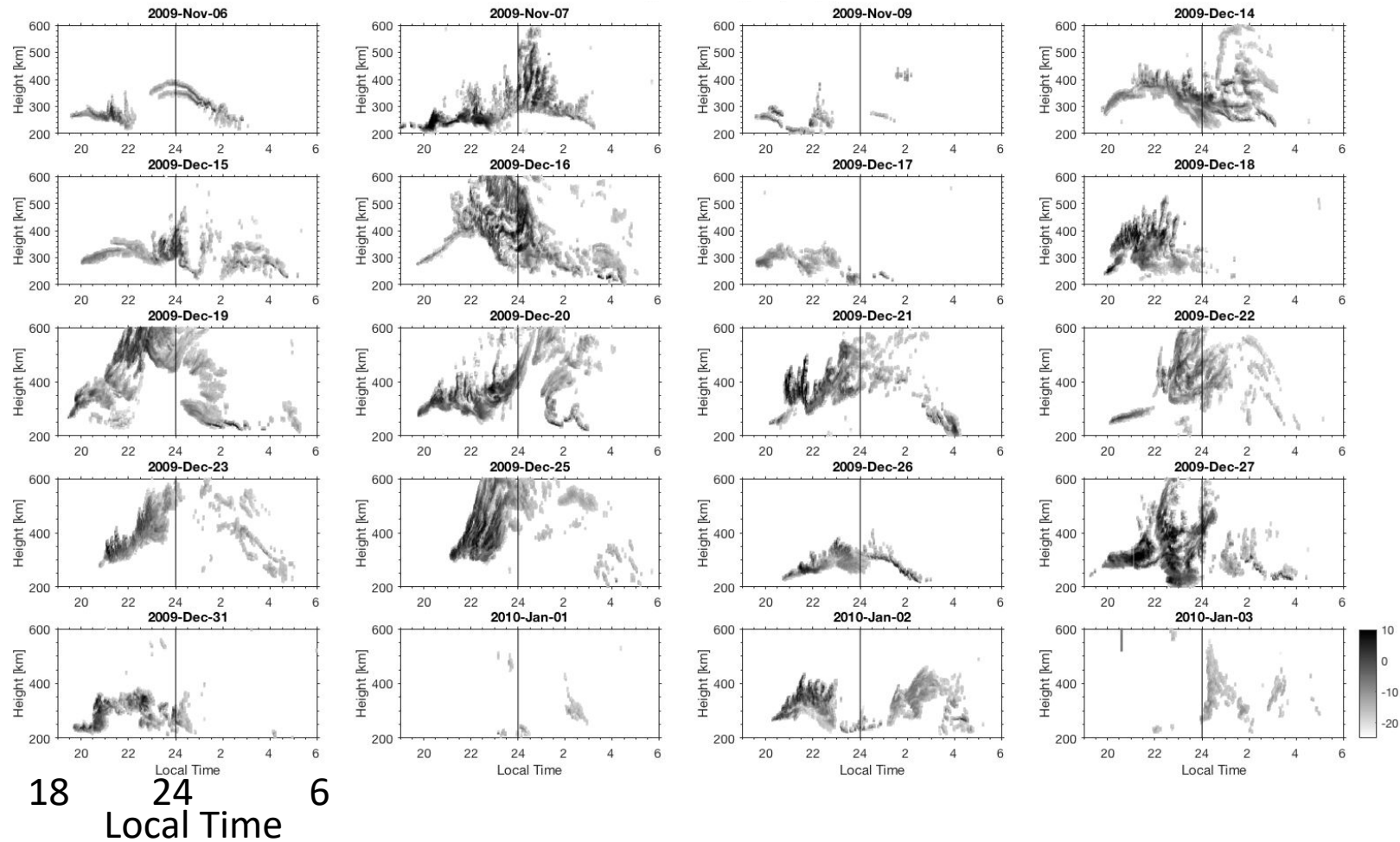


- June Solstice ESF: *F*-region conditions
- ✓ No clear signatures of PRE or midnight upward drifts
- ✓ ESF events are, however, often preceded by weak apparent uplifts

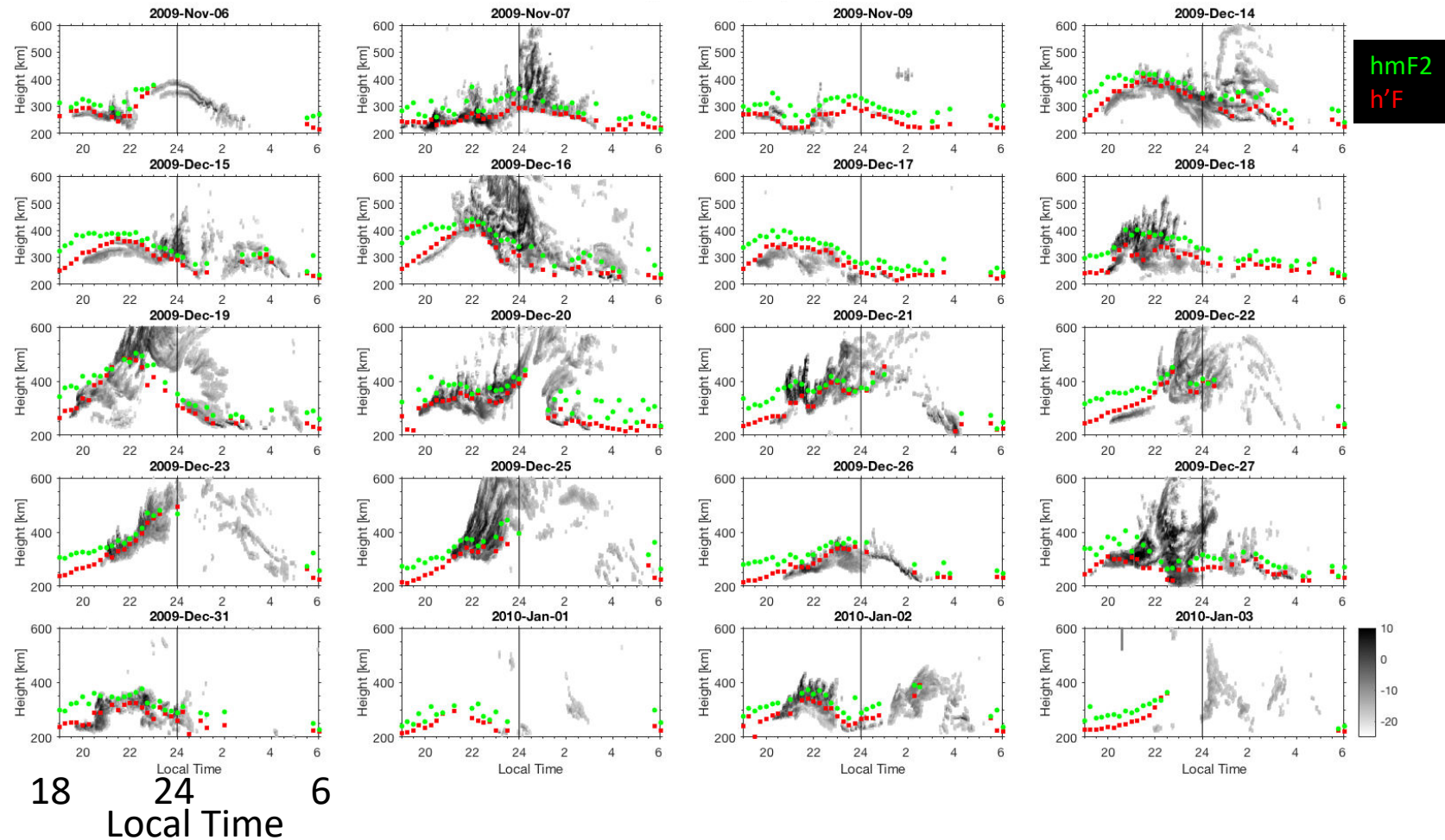


- December Solstice ESF: Morphology
- ✓ ESF starts in the evening and extends until post-midnight hours

RTI map

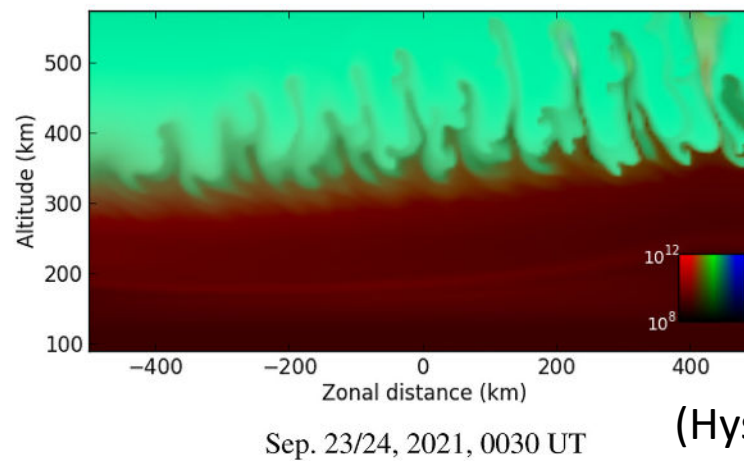
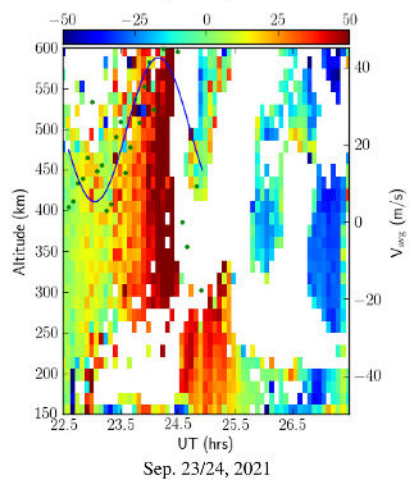
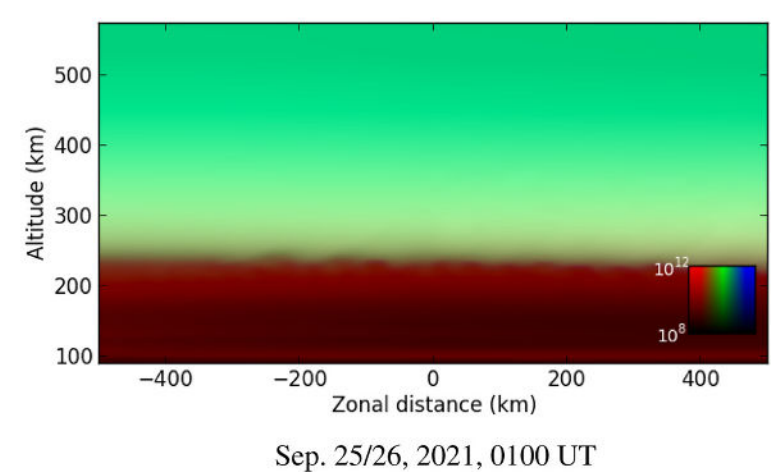
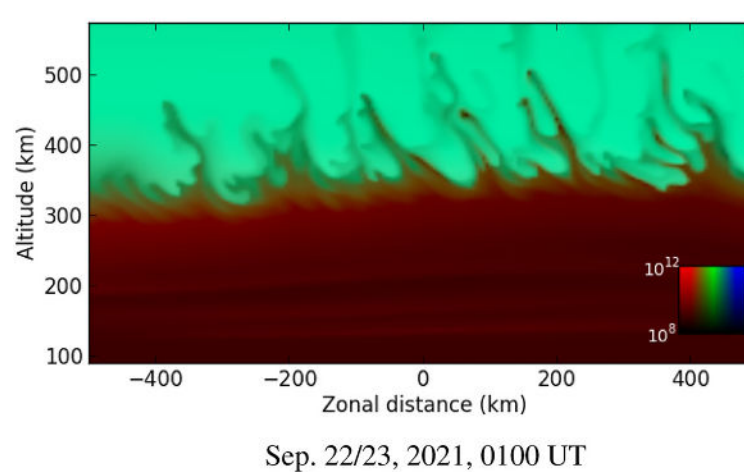
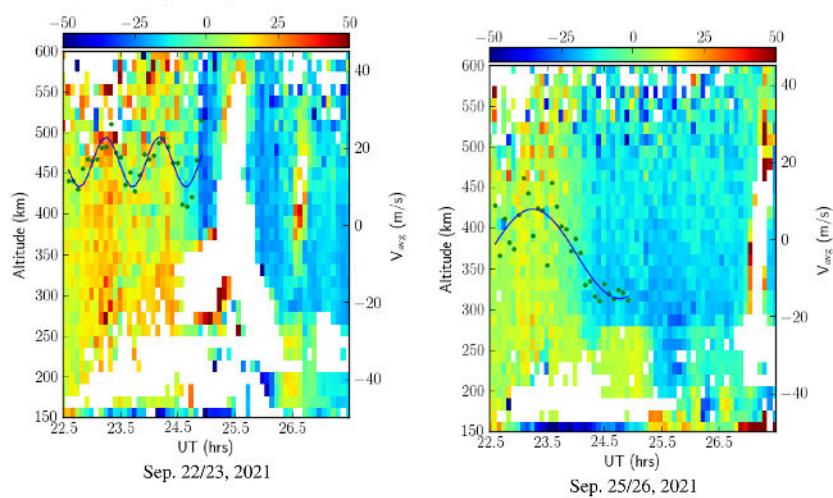
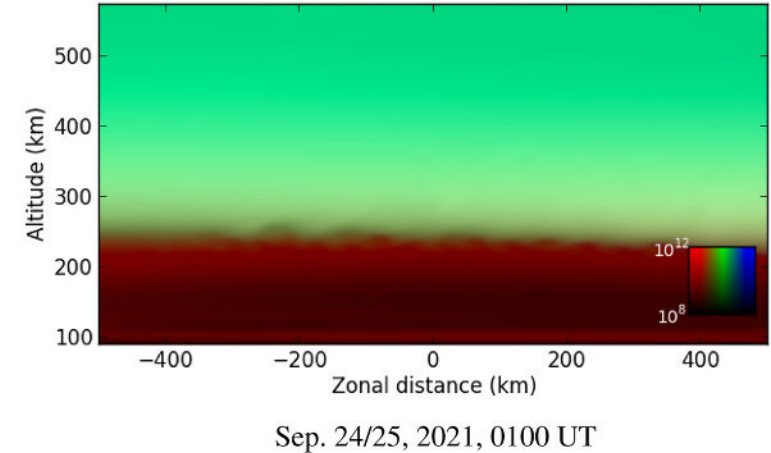
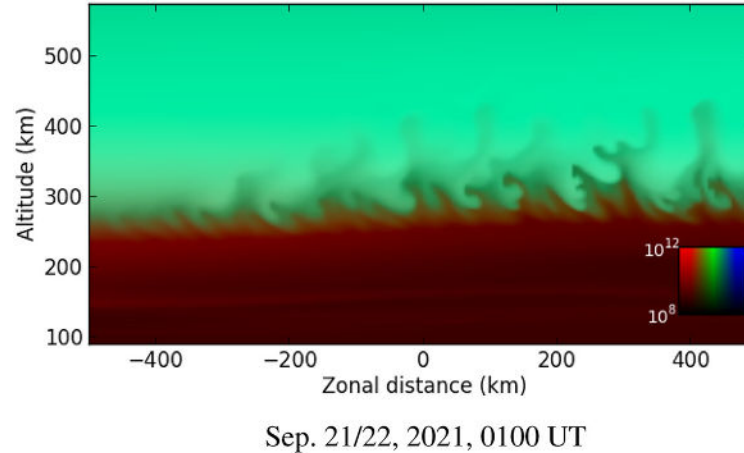
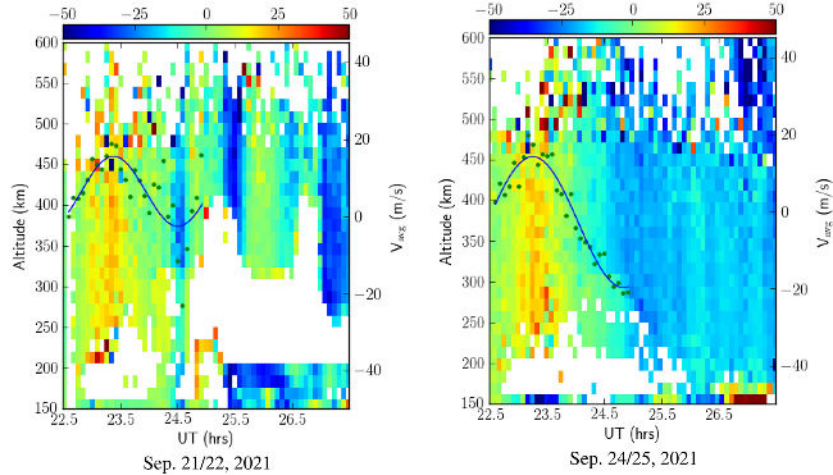


- December Solstice ESF: *F*-region conditions
- ✓ Signatures of PRE or late evening upward drifts
- ✓ Strong uplifts produce well-developed, long-lasting ESF events



Open questions

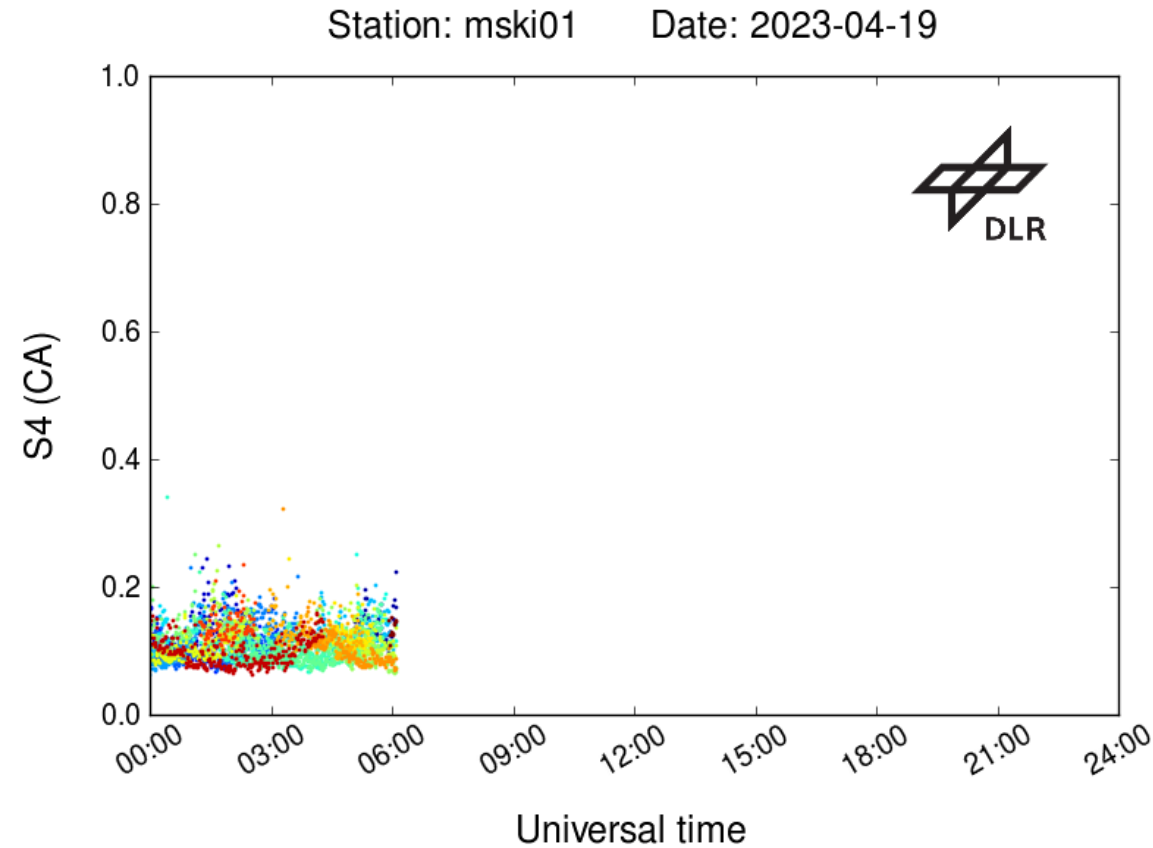
- 1. day-to-day variability
- 2. atypical ESF
- 3. prediction of occurrence



(Hysell et al., 2022)

Scintillation Index S4

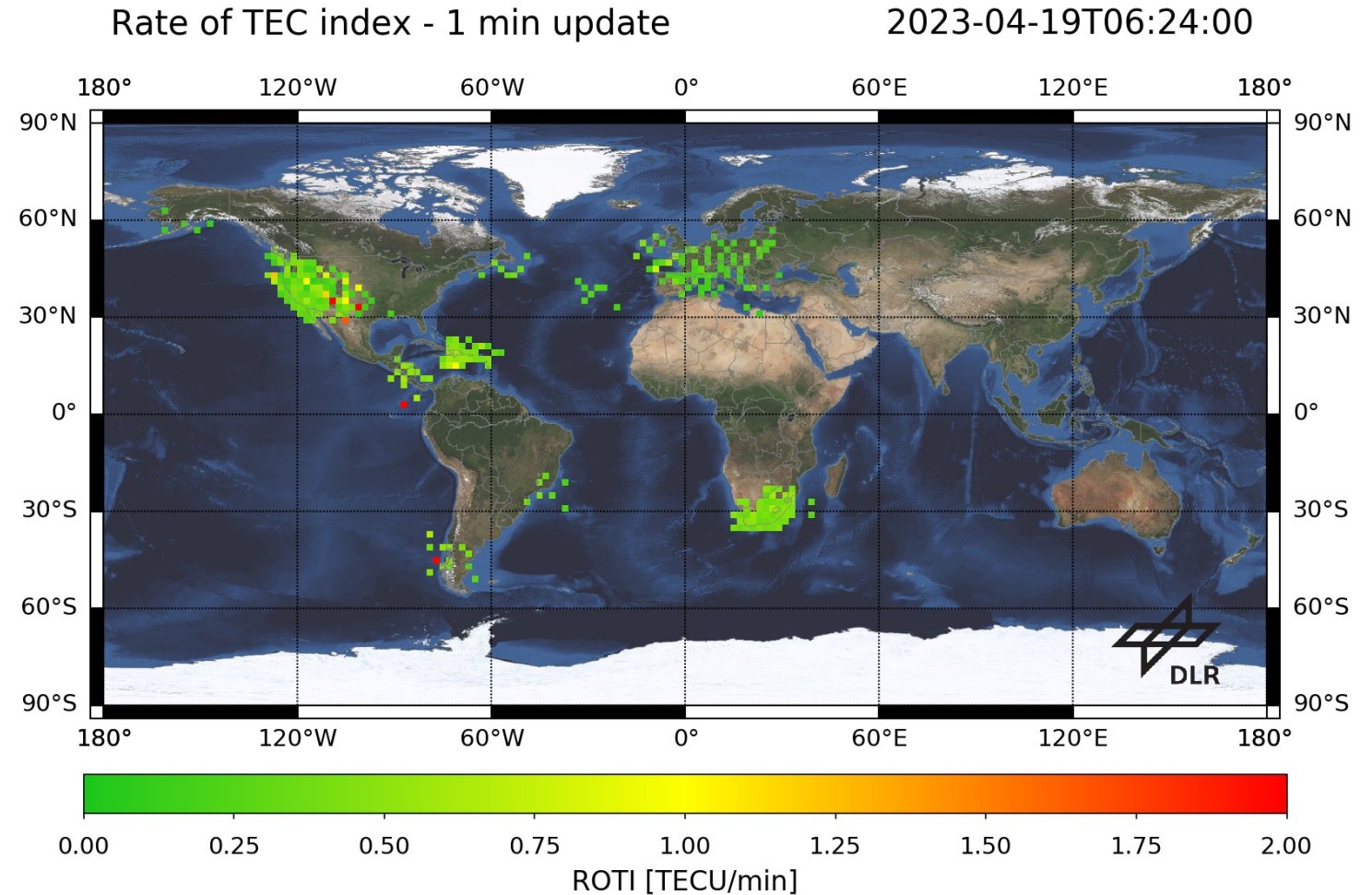
the normalized ratio of the standard deviation of signal intensity fluctuations to the mean signal intensity: $\frac{\langle I^2 \rangle - \langle I \rangle^2}{\langle I \rangle^2}$



https://swe.ssa.esa.int/tio_sci#

ROTI

- The Rate of TEC index (ROTI) is defined as standard deviation of the rate of TEC (ROT) assuming the ionosphere as a thin layer. Hence the index provides information about temporal ionospheric irregularities.



<https://impc.dlr.de/products/ionospheric-perturbations/rate-of-change-of-tec-index/one-minute-mean-roti-global>